

ANN-based energy reconstruction procedure for TACTIC γ -ray telescope and its comparison with other conventional methods

V.K.Dhar^{*}, A.K.Tickoo, M.K.Koul, R.C.Rannot, K.K.Yadav,
P.Chandra, B.P.Dubey[†], R.Koul

*Bhabha Atomic Research Centre,
Astrophysical Sciences Division.*

[†] *Electronics and Instruments Services Division,
Mumbai - 400 085, India.
Tel: 91-022-25593626*

Abstract

The energy estimation procedures employed by different groups, for determining the energy of the primary γ -ray using a single atmospheric Cherenkov imaging telescope, include methods like polynomial fitting in SIZE and DISTANCE, general least square fitting and look-up table based interpolation. A novel energy reconstruction procedure, based on the utilization of Artificial Neural Network (ANN), has been developed for the TACTIC atmospheric Cherenkov imaging telescope. The procedure uses a 3:30:1 ANN configuration with resilient backpropagation algorithm to estimate the energy of a γ -ray like event on the basis of its image SIZE, DISTANCE and zenith angle. The new ANN-based energy reconstruction method, apart from yielding an energy resolution of $\sim 26\%$, which is comparable to that of other single imaging telescopes, has the added advantage that it considers zenith angle dependence as well. Details of the ANN-based energy estimation procedure along with its comparative performance with other conventional energy reconstruction methods are presented in the paper and the results indicate that amongst all the methods considered in this work, ANN method yields the best results. The performance of the ANN-based energy reconstruction has also been validated by determining the energy spectrum of the Crab Nebula in the energy range 1-16 TeV, as measured by the TACTIC telescope.

Key words: Cherenkov imaging, TACTIC telescope, Artificial Neural Network, Energy reconstruction.

PACS: 95.55.Ka;29.90.+r

^{*} Corresponding author :
Email address: veer@barc.gov.in (V.K.Dhar).

1 Introduction

Very high energy (VHE) γ -ray astronomy, in the energy range $\sim 100\text{GeV}$ - 30TeV , has matured into an exciting field of research activity during the last decade [1-3]. The recent success of the field has mainly resulted from the development of the Cherenkov imaging technique [4-5] which allows efficient separation of photon induced showers from the hadron background. In this technique, the spatial distribution of photons in the image (called the Cherenkov image) is recorded by using a close-packed array of fast photomultiplier tubes (also called as the imaging camera with individual tubes as its pixels). By exploiting the subtle differences in the images produced by γ -ray and cosmic-ray initiated showers, caused by the physical processes responsible for the development of these showers in the atmosphere, it becomes possible to effectively segregate the two event species with a high degree of accuracy. The first success of the Cherenkov imaging technique was the detection of the Crab Nebula by the Whipple group in 1989 [6]. Following this landmark discovery a number of new experiments were set up (e.g. HEGRA, CAT, Durham Mark 6), leading to the discovery of more γ -ray sources. The HEGRA group were the first group to demonstrate that stereoscopic array of telescopes could improve the gamma/hadron discrimination even further. The progress achieved with new generation telescopes using either a single Cherenkov telescope (e.g. MAGIC [7]) or stereoscopic arrays (e.g. VERITAS [8], HESS [9] and CANGAROO [10]) has conclusively demonstrated that the imaging technique allows substantial removal of the cosmic ray background events, thereby yielding unprecedented sensitivity in the γ -ray energy range of 100GeV to 30TeV . It is primarily because of the success of these experiments that the field of ground-based γ -ray astronomy today boasts of a source catalogue of about 70 gamma-ray sources [3] from a variety of celestial objects including supernova remnants, pulsar wind nebulae, blazars, and microquasars.

Apart from detecting new γ -ray sources, one of the main aim of the Cherenkov imaging telescopes is to reconstruct the energy spectra of the sources. A study of the resulting spectral energy distributions can yield valuable information about the underlying γ -ray production mechanisms and unusual astrophysical environment characterizing these sources. In addition, differences in the observed energy spectrum of several active galactic nuclei can also be used to study absorption effects at the source or in the intergalactic medium due to the interaction of γ -rays with the extragalactic background photons [11,12].

Determining the energy of primary γ -rays is an important advantage which endows the atmospheric Cherenkov technique with calorimetric capability. While the light intensity in an image (also known as image SIZE), represents a key parameter for determining the energy of the primary γ -ray, one also has to consider its dependence on the core-position and zenith angle for improving the energy resolution. Since the precise information of core distance is not available with a single

imaging telescope, the energy resolution of these telescopes is generally limited to $\sim 25\text{-}35\%$ [13-15]. On the other hand, a stereoscopic system allows unambiguous reconstruction of the shower geometry including a direct measurement of core distance which leads to a significant increase in sensitivity and energy resolution of these systems [16,17].

The main aim of this work is to use an Artificial Neural Network (ANN) based procedure for estimating the energy of γ -ray like events, recorded by a single imaging telescope, on the basis of their image SIZE, DISTANCE and zenith angle. Apart from being used for classification (pattern recognition) purposes, ANN has also been applied extensively to problems like function approximation or regression analysis. The feasibility of employing ANN for pattern recognition problems in particle physics has been studied by a number of workers including separating gluon from quark jets [18] and identification of the decays of the Z^0 boson into $b\bar{b}$ pairs [19]. A feed-forward ANN classifier, used by the DELPHI collaboration, for separating hadronic decays of the Z^0 into c and b quark pairs has also yielded very promising results [20]. Superior performance of the neural network approach, as compared to other multivariate analysis methods including discriminant analysis and classification trees, has been reported for tagging of $Z^0 \rightarrow b\bar{b}$ events at LEP/SLC [21]. The feasibility of employing ANN for energy reconstruction has also been studied for a number of other applications (which are not related to Cherenkov imaging) and we will only refer here to few of these. While the Wizard collaboration has used it for GILDA imaging silicon calorimeter [22], the ANN-based approach has also been used for reconstruction of the energy deposited in the calorimetry system of the CMS detector [23] and the hadronic calorimeter of ATLAS, Tilecal [24].

Application of ANN to atmospheric Cherenkov imaging data, for distinguishing between γ -ray and cosmic-ray generated Cherenkov events, has been studied by several workers [25-28]. Promising results have also been reported for the wave-front sampling telescope CELESTE [29] where the ANN method was used for not only discriminating γ -ray and cosmic ray generated Cherenkov events but also for determining the primary energy and the location of the shower core. A detailed case study comparing different multivariate classification methods (classification trees, kernel and nearest-neighbour methods, linear discriminant analysis, support vector machines, neural network etc.) has also been performed in [30] using Monte Carlo simulated data generated for the MAGIC telescope. Keeping in view the encouraging results reported in above cited literature, the main thrust of this work is to use ANN for determining the energy of the γ -rays detected by an atmospheric Cherenkov imaging telescope. While the basic idea of applying ANN for determining the energy of the γ -rays, from a point source, has already been used by us in recent past for determining the energy spectra of the Crab Nebula, Mrk-421 [31] and Mrk-501 [32], as measured by the TACTIC telescope, the emphasis in this work will be on presenting a detailed description of the ANN-based energy reconstruction methodology and its comparison with conventional methods. In addition,

the other two aspects which have been incorporated in the present work are the usage of more data for training (see Section 3 for more details), to achieve a lower normalized rms error, than reported in [31], and also to check the interpolation capability of the proposed ANN method with an independent data sample. Finally, the performance of the ANN-based energy reconstruction is validated by revisiting the energy spectrum of the Crab Nebula in the energy range 1-16 TeV as measured by the TACTIC telescope.

2 TACTIC telescope

The TACTIC (TeV Atmospheric Cherenkov Telescope with Imaging Camera) γ -ray telescope has been in operation at Mt. Abu (24.6° N, 72.7° E, 1300m asl), India, for the last several years to study TeV gamma ray emission from celestial sources. The telescope deploys a F/1 type tracking light collector of $\sim 9.5 \text{ m}^2$ area, made up of 34 x 0.6 m diameter, front-coated spherical glass facets which have been prealigned to produce an on-axis spot of $\sim 0.3^\circ$ diameter at the focal plane. The telescope uses a 349-pixel imaging camera, with a uniform pixel resolution of $\sim 0.3^\circ$ and a $\sim 6^\circ \times 6^\circ$ field-of-view, to record atmospheric Cherenkov events produced by incoming cosmic-ray particles or gamma-ray photons. The innermost 121 pixels (11×11 matrix) are used for generating the event trigger, based on the NNP (Nearest Neighbour Pairs) topological logic [33], by demanding a signal ≥ 25 pe for the 2 pixels which participate in the trigger generation. The back-end signal processing hardware of the telescope is based on NIM and CAMAC modules developed inhouse. The data acquisition and control system of the telescope [34] has been designed around a network of PCs running the QNX (version 4.25) real-time operating system. The triggered events are digitized by CAMAC based 12-bit Charge to Digital Converters (CDC) which have a full scale range of 600 pC. The relative gain of the photomultiplier tubes is monitored by repeatedly flashing a blue LED, placed at a distance of $\sim 1.5\text{m}$ from the camera. The data acquisition and control of the TACTIC is handled by a network of three PCs. While one PC is used to monitor the scaler rates and control the high voltage to the photomultipliers, the other PC handles the acquisition of the atmospheric Cherenkov events and LED calibration data. These two front-end PCs, referred to as the rate stabilization node and the data acquisition node respectively, along with a master node form the multinode Data Acquisition and Control network of the TACTIC Imaging telescope. All executable routines stored on the master node are spawned on to the other two front-end nodes as and when required. The telescope has a pointing and tracking accuracy of better than ± 3 arc-minutes. The tracking accuracy is checked on a regular basis with so called "point runs", where an optical star having its declination close to that of the candidate γ -ray source is tracked continuously for about 5 hours. The point run calibration data (corrected zenith and azimuth angle of the telescope when the star image is centered) are then incorporated in the telescope

drive system software so that appropriate corrections can be applied directly in real time while tracking a candidate γ -ray source.

Operating at γ -ray threshold energy of ~ 1.2 TeV, the telescope records a cosmic ray event rate of ~ 2.0 Hz at a typical zenith angle of 15° . The telescope has a 5σ sensitivity of detecting the Crab Nebula in 25 hours of observation time and has so far detected γ -ray emission from the Crab Nebula, Mrk 421 and Mrk 501. Details of the instrumentation aspects of the telescope and some of the results obtained on various candidate γ -ray sources are discussed in [31-35].

3 Monte Carlo simulations for energy reconstruction of γ -rays

The Monte Carlo simulation data used for developing a procedure for energy reconstruction of γ -rays are based on the CORSIKA (version 5.6211) air-shower simulation code [36]. The simulated data-base for γ -ray showers used about 34000 showers in the energy range 0.2-20 TeV with an impact parameter of upto 250m. These showers have been generated at 5 different zenith angles ($\theta = 5^\circ, 15^\circ, 25^\circ, 35^\circ$ and 45°). A data-base of about 39000 proton initiated showers in the energy range 0.4-40 TeV, were used for studying the gamma/hadron separation capability of the telescope and confirming the matching between experimental and simulated image parameter distributions. The incidence angle of the proton showers was simulated by randomizing the arrival direction of the primary in a field of view of $6^\circ \times 6^\circ$ around the pointing direction of the telescope. Wavelength dependent atmospheric absorption, the spectral response of the PMTs and the reflection coefficient of mirror facets and light cones has also been taken into account while performing the simulations. The number of photoelectrons registered by each pixel has then been subjected to noise injection, trigger condition check and image cleaning. The clean Cherenkov images were characterized by calculating their standard image parameters like LENGTH, WIDTH, DISTANCE, ALPHA, SIZE and FRAC2 [4,5]. The same simulation data base has also been used, as per the well known standard procedure, for calculating the effective area of γ -rays as a function of energy and zenith angle and, also the γ -ray retention factors when Dynamic Supercuts are applied to the simulated data. Both these inputs are required for determining the energy spectrum of a source once a statistically significant γ -ray signal is observed in the data.

Keeping in view the fact that the Cherenkov light emitted from the electromagnetic cascade is to a first order approximation proportional to the energy of the primary γ -ray, the approach followed in atmospheric Cherenkov imaging telescopes is to determine the energy on the basis of the image SIZE. Since the intensity of the Cherenkov light is a function of core distance, which is not possible to obtain with a single imaging telescope, the angular distance of the image centroid from the camera center (known as the DISTANCE parameter) is generally used as an ap-

proximate measure of the impact distance. The energy reconstruction procedure with a single imaging telescope thus involves using SIZE and DISTANCE parameters of the Cherenkov event for determining energy of the primary γ -ray. Although the method has been found to work reasonably well over a restricted zenith angle range of $\leq 30^\circ$, there is a need to include zenith angle dependence in the energy reconstruction procedure for allowing data collection over a much wider zenith angle range.

In order to check the performance of various energy reconstruction procedures for the TACTIC telescope, we have divided the simulated data base into two parts so that one part could be used for preparing the data for obtaining parameterized fits (or training the ANN) and the remaining for testing. For smoothening event to event fluctuation, which are inherently present in raw data, we have first calculated $\langle \text{SIZE} \rangle$ and $\langle \text{DISTANCE} \rangle$ by clubbing together showers of a particular energy in various core distance bins with each bin having a size of 40m. Furthermore, additional selection criteria (viz., accepting events with core distance $> 30\text{m}$, $\text{SIZE} > 50\text{pe}$ and DISTANCE between 0.4° to 1.4°) has also been used while preprocessing the training data to ensure that the image is robust with minimum possible truncation effects. Imposing a lower bound on the core distance helps in rejecting the events where shower to shower fluctuations in the light intensity are expected to be very large, as most of the light in this region is produced by local penetrating particles whose number can vary quite widely. The final training data file thus consists of a single table with ~ 350 rows. Each row has 4 columns with one column each for energy, $\langle \text{SIZE} \rangle$, $\langle \text{DISTANCE} \rangle$ and zenith angle. It is worth mentioning here that although the raw data used for training is same as used in [31], there is a slight difference in the procedure followed for preparing the training data file in this work. Using the same number of showers as used in the previous work (i.e 10,000), a new training data file of 350 events (as against 200 events used by us in our earlier work [31]) was generated by interpolating $\langle \text{SIZE} \rangle$ at $\langle \text{DISTANCE} \rangle$ values of 0.40° , 0.50° 1.40° for each energy and zenith angle. A representative example of the variation of $\langle \text{SIZE} \rangle$ as a function of $\langle \text{DISTANCE} \rangle$ for different primary γ -ray energies is shown in Fig.1. It is quite evident from this figure that SIZE (proportional to the Cherenkov light in an image) is the most important factor which needs to be considered for estimating the energy of the primary γ -ray. Since, for a fixed γ -ray energy, $\langle \text{SIZE} \rangle$ also depends on core distance (proportional to DISTANCE parameter of the image for a point γ -ray source) the second factor which needs to be considered is the DISTANCE parameter. On comparing Fig.1a and Fig.1b, which show the behaviour of $\langle \text{SIZE} \rangle$ at zenith angles of 15° and 35° , respectively, one finds that the zenith angle dependence cannot be ignored in situations where a wider zenith angle coverage is required.

The performance of a particular energy reconstruction procedure has been evaluated by calculating the relative error in the reconstructed energy (Δ_E), for individual γ -ray events using the test data file. The relative error in the reconstructed en-

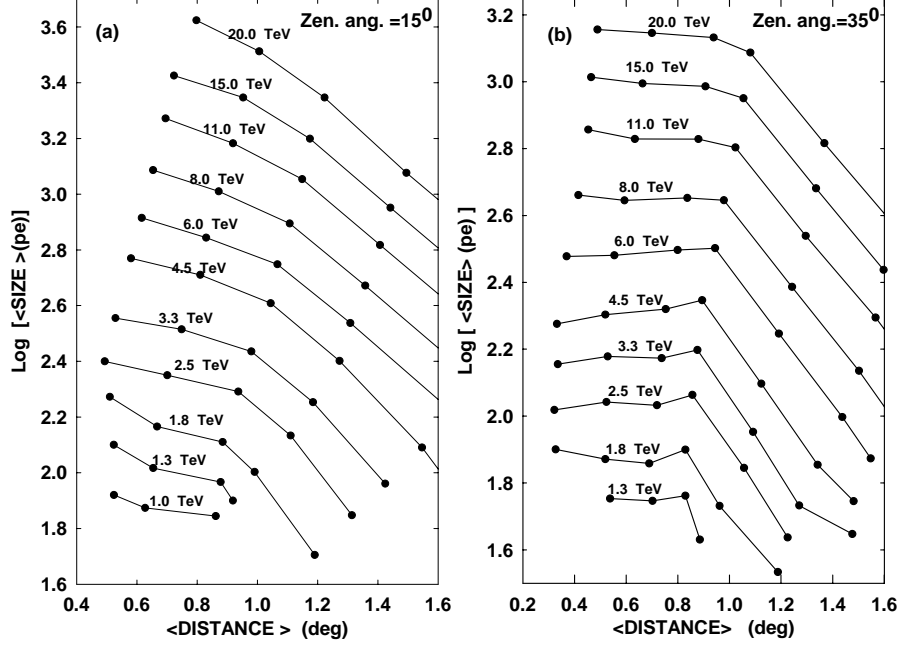


Fig. 1.

ergy is defined as $(E_{estm} - E_{true})/E_{true}$, where E_{true} is the true energy and E_{estm} is the estimated energy yielded by the energy reconstruction procedure. The mean value of (Δ_E) as a function of E_{true} and energy resolution $(\sigma(\Delta_E))$ defined as the root mean square width of the distribution of Δ_E are the main quantities which can be used for comparing the performance of various energy reconstruction procedures. It is worth mentioning that the energy resolution, is sometimes estimated by calculating rms width of the distribution of $\ln(E_{true}/E_{estm})$ [13,31] or $\ln(E_{estm}/E_{true})$ [37]. The only reason for using $(E_{estm} - E_{true})/E_{true}$ in this work as against $\ln(E_{estm}/E_{true})$ is to follow a more standard and widely accepted definition of energy resolution [38]. Nevertheless, it can be easily shown that $(E_{estm} - E_{true})/E_{true} \sim \ln(E_{estm}/E_{true})$.

4 Conventional energy reconstruction methods

4.1 Parameterized fit with DISTANCE and SIZE as variables

The first energy estimation procedure which has been studied here is based on the approach followed by Whipple group [13, 15], where $\ln(E_{estm})$ is expressed as a polynomial in $\ln(\text{SIZE})$ and DISTANCE . The approach assumes that, for a point γ -ray source, DISTANCE parameter of the image provides an approximate measure of the core distance. The validity of this assumption has also been checked for

the TACTIC telescope simulation data and the results of the same are presented in Fig.2.

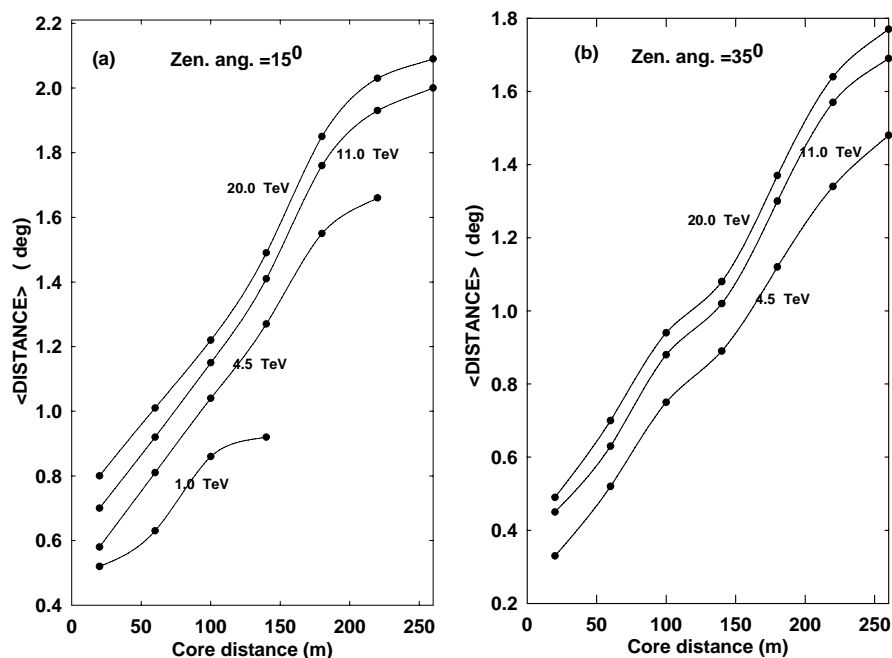


Fig. 2.

The data used in this figure has been generated by clubbing together showers of a particular energy in various core distance bins with each bin having a size of 40m and finding $\langle \text{DISTANCE} \rangle$ for each core distance bin. Although a strong correlation between core distance and $\langle \text{DISTANCE} \rangle$ is clearly visible in Fig.2, it is worth mentioning here that DISTANCE parameter of a Cherenkov image produced by an individual shower is also dependent on the height of the shower maximum [39]. Since for a single telescope it is impossible to determine separately the core distance and height of shower maximum on an event to event basis, obtaining an approximate measure of the core distance on the basis of DISTANCE parameter seems to be the only viable solution. Ignoring zenith angle dependence and following the Whipple procedure, E_{estm} , based on image SIZE (S) and DISTANCE (D) is calculated by using the following relation

$$\ln(E_{estm}) = a_1 + a_2 \ln(S) + a_3 (\ln(S))^2 + a_4(D_0) + a_5(D_0)D \quad (1)$$

Choosing $D_0=1.00^\circ$, the values of a_1 , a_2 , a_3 , $a_4(D_0)$ and $a_5(D_0)$, obtained after fitting equation (1) to the training data file at zenith angle of 25° , are found out to be the following : $a_1 \sim -2.8820$, $a_2 \sim 0.7221$, $a_3 \sim 0.0035$, $a_4(D \leq D_0) \sim -0.2005$, $a_5(D \leq D_0) \sim 0.2395$, $a_4(D > D_0) \sim -1.6766$ and $a_5(D > D_0) \sim 1.7290$. While the first 3 terms in the above equation use the fact that total intensity of an image is roughly proportional to the energy of the primary, the remaining 2 terms modify

this relationship by including the dependence on the core distance also. A plot of relative error in the energy reconstruction obtained for test data sample at zenith angle 25° is shown in Fig.3a.

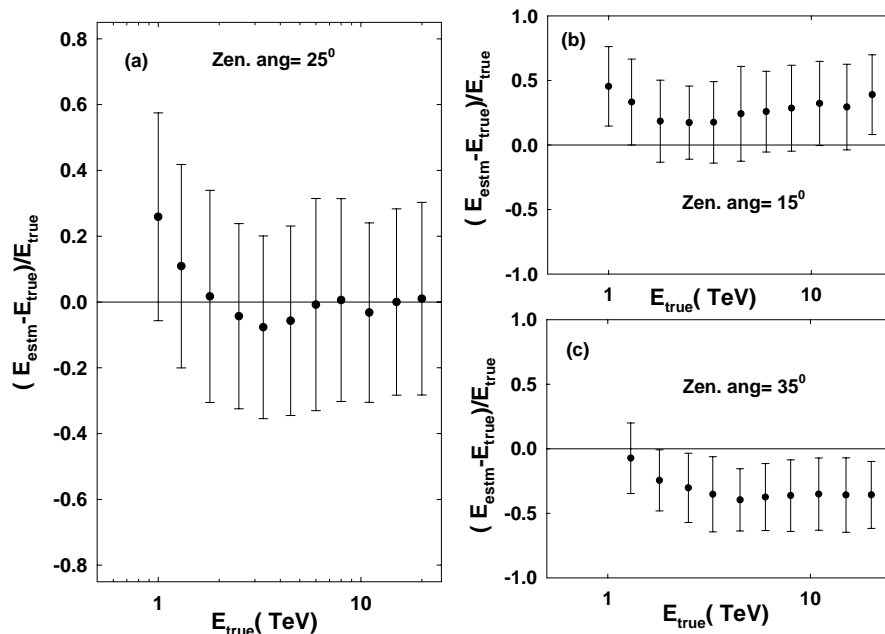


Fig. 3.

The corresponding relative error in the reconstructed energy (Δ_E) for zenith angle of 15° and 35° is also shown in (b) and (c) if zenith angle dependence is ignored and fit coefficients obtained at zenith angle of 25° are used as such in the energy reconstruction procedure at the other two zenith angles also. Although the energy reconstruction procedure yields $\sigma(\Delta_E) \sim 28\%$ for the data shown in Fig.3a, presence of a systematic bias seen in Fig.3b and Fig.3c ($\sim 20\%$ and $\sim -37\%$ at zenith angles of 15° and 35° , respectively) suggests that there is a need to include zenith angle dependence in the energy reconstruction procedure for allowing data collection over a much wider zenith angle range.

4.2 Parameterized fit with *DISTANCE*, *SIZE* and zenith angle as variables

Including the zenith angle (z) dependence, in the energy construction procedure, can be in principle implemented by adding one or more zenith angle dependent terms to equation (1). The method followed here uses guidance from [40] and employs the following relation for estimating the energy.

$$\ln(E_{estm}) = 1.0 + b_1 \ln(S) + b_2 \sqrt{\ln(S)} + b_3 (\ln(S))^2 + b_4 / \cos(z) + b_5 D \quad (2)$$

The values of the constants after fitting equation (2) to the training data file at all the 5 zenith angles (i.e 5° , 15° , 25° , 35° and 45°) together are found out to be following : $b_1 \sim 4.0053$, $b_2 \sim -9.7814$, $b_3 \sim -0.1029$, $b_4 \sim 3.3510$ and $b_5 \sim 0.7822$. Plot of relative error in the estimated energy as a function of energy for the test data sample at all 5 zenith angles is shown in Fig.4a.

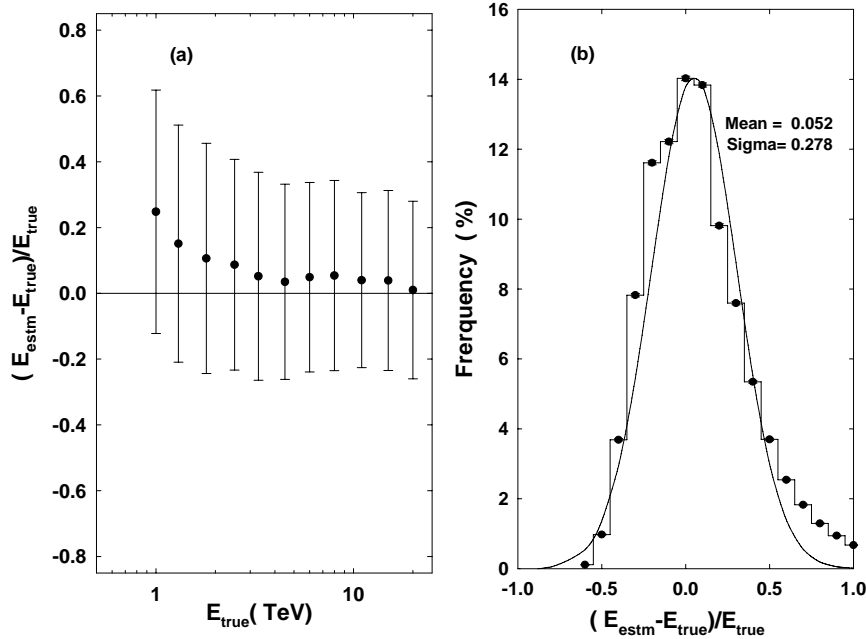


Fig. 4.

Frequency distribution of Δ_E by considering almost equal number showers at different energies is shown in Fig.4b. The root mean square width of the distribution is $\sim 31\%$ and the same for the fitted Gaussian distribution is $\sim 28\%$. Systematic bias at all energies ($\sim 7\%$ in the energy range 1.8 TeV to 15.0 TeV) is also seen in Fig.4a which suggests that actual zenith angle dependence in the energy reconstruction procedure is probably more complicated than what has been considered in equation (2). An improvement in the energy resolution has been reported in [40] by including an additional parameter called LEAKAGE (defined as the ratio of light content in the edge pixels to total light content or SIZE) in equation (2), to compensate for leakage effects in the relatively small ($\sim 3^\circ$ diameter) HEGRA CT1 camera. Since the TACTIC telescope uses a fairly large camera ($\sim 6^\circ$ diameter) we do not expect the energy resolution to improve if LEAKAGE parameter is also used. However, an attempt to remove the systematic bias was also tried by using a nonlinear model with 2 more zenith angle dependent terms (viz., $D/\cos(z)$ and D

$\ln(S)/\cos(z)$) in equation (2), but the improvement was found to be only marginal. It is worth mentioning here that while the method of least squares often gives optimal estimates of the unknown parameters, it is very sensitive to the presence of unusual data points in the data used to fit a model. One or two outliers can sometimes seriously skew the results of a least squares analysis.

4.3 *Look-up table method using interpolation in 3 dimensions*

The third energy reconstruction method which has been studied here is based on the look-up table method. This method has been used quite extensively by the HEGRA collaboration [39]. Although the method was originally developed for the HEGRA stereoscopic array, we essentially follow the same principle here. In this method, we generate the fine grid look-up table by using the training data file. This is done by interpolating the expected $\langle \text{SIZE} \rangle$ at finer intervals of DISTANCE, energy and zenith angle. The total number of interpolated SIZE values, at a particular zenith angle, comprise ~ 4000 values with DISTANCE parameter ranging from 0.4° to 1.4° and energy values ranging from ~ 0.74 TeV to ~ 20 TeV. In order to perform interpolation in zenith angle, 9 different data files are prepared at 5° interval in the zenith angle range from 5° to 45° . While the above interpolated data has been obtained by fitting polynomial curves of order 3 to the given data points, final energy estimation of an event, on the basis of its SIZE, DISTANCE and zenith angle, uses only linear interpolation. Plot of the relative mean error in the reconstructed energy (Δ_E) as a function of energy for test data sample at all the 5 zenith angles is shown in Fig.5a. The frequency distribution of Δ_E is shown in Fig.5b.

It is quite evident from Fig.5a that, barring energy values at 1.0 TeV, 1.3 TeV and 20.0 TeV where $|\Delta_E|$ is found to be $>5.0\%$, the reconstructed energy has a negligible bias at other energy values from 1.8 TeV to 15.0 TeV. The rms width of the frequency distribution is found to be $\sim 27\%$ and the rms width of the fitted Gaussian distribution is $\sim 24\%$. It is important to mention here that a positive bias seen in the relative mean error (Fig.3a, Fig.4a and Fig.5a) at energy values of 1.0 TeV and 1.3 TeV is because of the well known selection effect [39] and is due to sub-threshold regime event triggers because of their upward fluctuations in the light yield sometimes. Since events with downward fluctuations in the light yield are unable to trigger the system in this energy range, the energy estimates tend to be biased towards larger values.

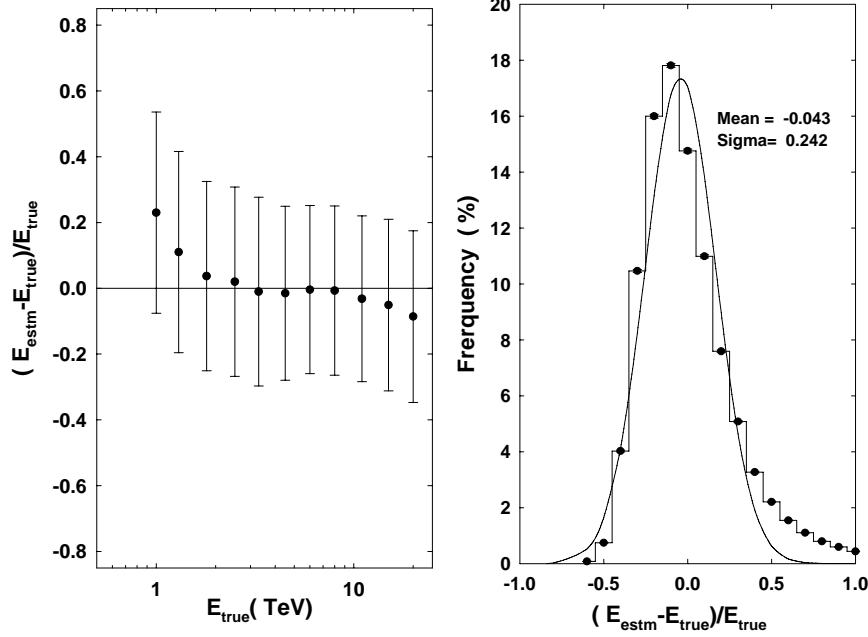


Fig. 5.

5 Energy reconstruction using Artificial Neural Network

5.1 Overview of ANN and training of the network

An artificial neural network (ANN) is an interconnected group of artificial neurons that uses a mathematical model for information processing to accomplish a variety of tasks. They can be configured in various arrangements to perform a range of tasks including pattern recognition and classification. In more practical terms, an ANN is a non-linear data modeling tool which can be used to model complex relationships between inputs and outputs or to find patterns in the data. The ability of ANN to handle non-linear data interactions, and their robustness in the presence of high noise levels has encouraged their successful use in diverse areas of physics, biology, medicine, agriculture, computer research and astronomy [41]. In a feed-forward ANN the network is constructed using layers where all nodes in a given layer are connected to all nodes in a subsequent layer. The network requires at least two layers, an input layer and an output layer. In addition, the network can include any number of hidden layers with any number of hidden nodes in each layer. The signal from the input vector propagates through the network layer by layer till the output layer is reached. The output vector represents the predicted output of the ANN and has a node for each variable that is being predicted. The task of training the ANN is to find the most appropriate set of weights for each connection which minimizes the output error. All weighted-inputs are summed at the neuron node and this summed

value is then passed to a transfer (or scaling) function. For a feed-forward network with K input nodes described by the input vector (x_1, x_2, \dots) , one hidden layer with J nodes and I output nodes, the output F_i is given by the following equation

$$F_i = g \left[\sum_{j=1}^J w_{ij} g \left(\sum_{k=1}^K w_{jk} x_k + \theta_j \right) + \theta_i \right] \quad (3)$$

where w_{ij}, w_{jk} are the weights, θ_i, θ_j are the thresholds and $g(*)$ is the activation function. The training data sample is repeatedly presented to the network in a number of training cycles, and the adjustment of the free parameters (w_{ij}, w_{jk}, θ_i and θ_j) is controlled by the learning rate η . The essence of the training process is to iteratively reduce the error between the predicted value and the target value. While the choice of using a particular error function is problem dependent, there is no well defined rule for choosing the most suitable error function. We have used the normalized root-mean-squared error S_{rms} [42] in this work which is defined as :

$$S_{rms} = \frac{1}{PI} \sqrt{\frac{1}{2} \sum_{p=1}^P \sum_{i=1}^I \left(\frac{D_{pi} - O_{pi}}{D_{pi}} \right)^2} \quad (4)$$

where D_{pi} and O_{pi} are the desired and the observed values and P is number of training patterns. The error here depicts the accuracy of the neural network mapping after a number of training cycles have been implemented.

Given the inherent power of Artificial Neural Network (ANN) to effectively handle the multivariate data fitting, we have developed an ANN-based energy estimation procedure for determining the energy of the primary γ -ray on the basis of its image SIZE, DISTANCE and zenith angle. The procedure followed by us uses a 3:30:1 (i.e 3 nodes in the input layer, 30 nodes in hidden layer and 1 node in the output layer) configuration of the ANN with resilient back propagation training algorithm [43] to estimate the energy of a γ -ray event on the basis of its image SIZE, DISTANCE and zenith angle. The 3 nodes in the input layer correspond to zenith angle, SIZE and DISTANCE, while the 1 node in the output layer represents the expected energy (in TeV) of the event. As already mentioned earlier, the training data comprises \sim 350 events where \langle SIZE \rangle and \langle DISTANCE \rangle are first obtained at each zenith angle by clubbing together showers of a particular energy in various core distance bins. Apart from reducing the training data base, following this method also makes ANN training simpler for achieving the desired level of convergence in a reasonable amount of time. The activation function chosen for the present study is the sigmoid function. In order to optimize the number of nodes required in the hidden layer, we also varied the number of the nodes in the hidden layer from 5 to 60 in steps of 5. A plot of the normalised rms error as a function of number of nodes in the hidden layer is shown in Fig.6a.

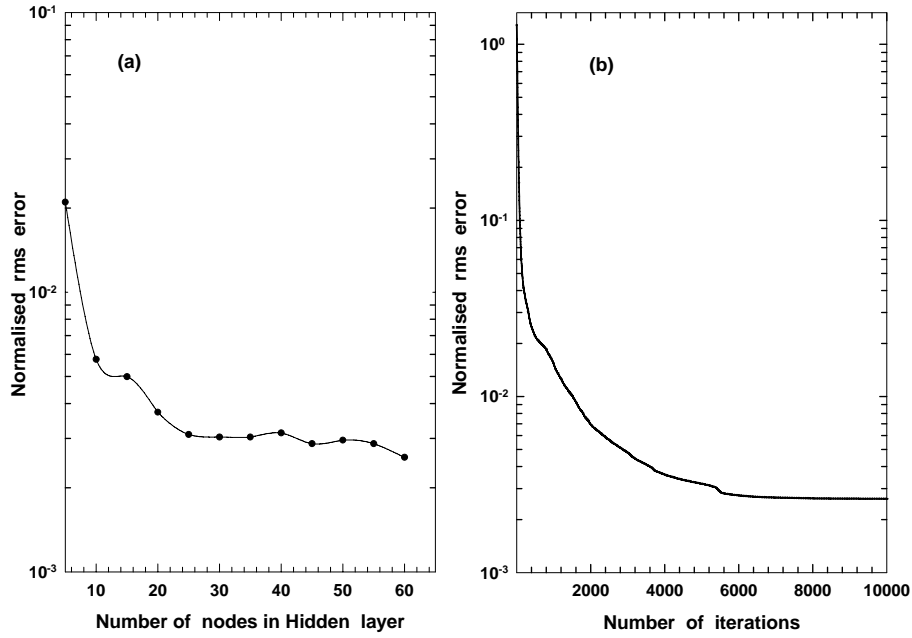


Fig. 6.

Since by increasing the number of nodes beyond 30 results in only a marginal reduction in the normalised rms error (at the cost of higher computation time), it seems one hidden layer with 30 nodes is quite optimum. The normalised rms error at the end of the training, for 30 nodes in the hidden layer, reaches a value $\sim 3 \times 10^{-3}$ and variation of the same as a function of number of iterations is shown in Fig.6b. It is worth mentioning here that a normalised rms error of $\sim 2.7 \times 10^{-2}$ was achieved in our previous work [31] and the improvement seen in the present work is as a result of using more data during ANN training. In order to ensure that the network has not become "over-trained" [44], the ANN training is stopped when the normalised rms error stops decreasing any further (somewhere around 8000 iterations).

5.2 Testing and validation of the ANN

The ANN is tested with two data samples. The first data sample comprises 10,000 gamma-ray images (which was earlier used for calculating mean SIZE and mean DISTANCE while preparing the training data set). The second data sample comprises 24,000 gamma-ray images which were not used at all while preparing the training data set. Both these data samples yielded similar energy reconstruction error plots, thus indicating that ANN has "learned" and not "remembered" the energy reconstruction procedure through over-training [44]. Plot of energy reconstruction error obtained for second test data sample is shown in Fig.7a. The frequency distri-

bution of Δ_E is shown in Fig.7b.

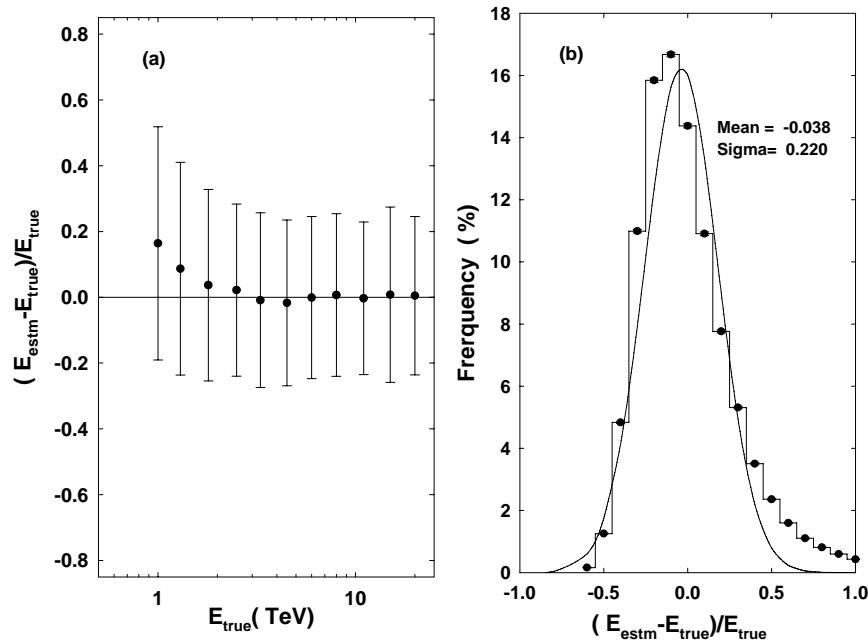


Fig. 7.

It is evident from Fig.7a that, the reconstructed energy, employing the ANN method, has a negligible bias in the energy range 1.8 TeV to 20.0 TeV with $|\Delta_E| < 5.0\%$. The rms width of the frequency distribution is found to be $\sim 26\%$ and the same for best fit Gaussian distribution is $\sim 22\%$.

The interpolation capability of the ANN-based energy reconstruction procedure, at intermediate γ -ray energies and zenith angles, has also been checked by applying it to an independent validation data base of 4000 showers. The energy of the primary γ -rays was chosen to be 1.1 TeV, 2.1 TeV, 5.2 TeV and 9.5 TeV at zenith angles of 10° and 20° , and 2.1 TeV, 5.2 TeV, 9.5 TeV and 17.0 TeV at zenith angles of 30° and 40° . Since no simulated data at these zenith angles and energies was used during training of the ANN, the results obtained now on the validation data obviously indicate the interpolation capability of the ANN. A plot of energy reconstruction error obtained for the validation data sample is shown in Fig.8a. The frequency distribution of Δ_E along with a best fit Gaussian distribution to the histogram is shown in Fig.8b.

The rms width of the best fit Gaussian distribution for the test and validation data ($\sim 22\%$ and $\sim 26\%$, respectively), with a negligible bias in the energy suggests that the performance of the ANN-based method energy reconstruction is quite reliable. Taking higher of the two $\sigma(\Delta_E)$ values (i.e $\sigma(\Delta_E) \sim 26\%$) as a safe value of the energy resolution achieved by the ANN-based energy reconstruction procedure, one

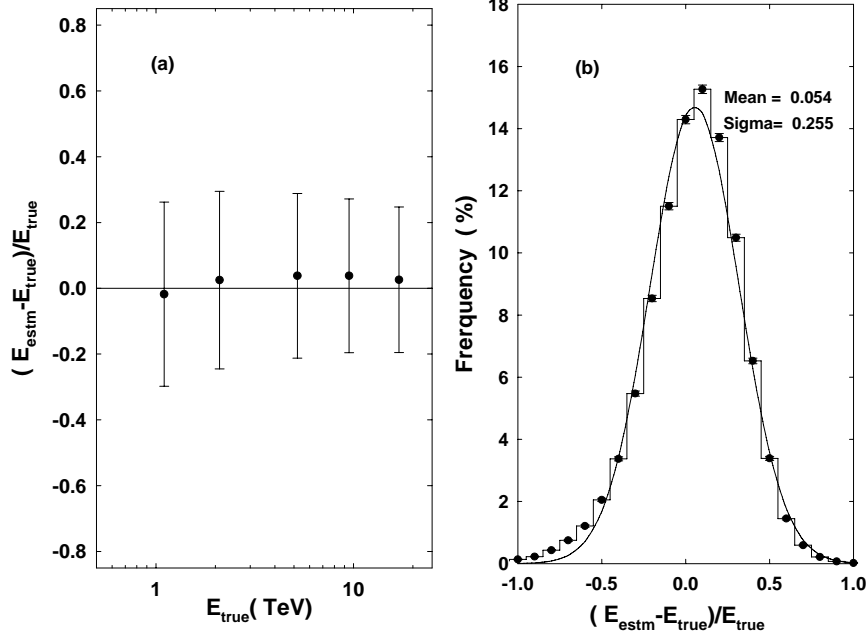


Fig. 8.

can easily conclude that the proposed method, apart from yielding a comparable performance to that of other single imaging telescopes (e.g. $\sigma(\ln E)$ of $\sim 25\%$ reported by the Whipple group [15]), has the added advantage that it considers zenith angle dependence of SIZE and DISTANCE parameters as well. The procedure thus allows data collection over a much wider zenith angle range as against a coverage of upto 30° in case the zenith angle dependence is to be ignored. On analyzing figures 3, 4, 5 and 7, it is also obvious that the ANN-based energy reconstruction procedure yields better results (both in terms of bias and energy resolution) as compared to the conventional energy reconstruction methods. Even though the look-up table based energy reconstruction procedure appears to be equally competitive it suffers from other drawbacks. Implementation of this method requires cumbersome tabulation of interpolated data at a number of DISTANCE, energy and zenith angle values and energy reconstruction procedure is also more time consuming as compared to the ANN method. Implementation of the ANN-based energy reconstruction procedure, on the other hand, is relatively much more straight forward. Once satisfactory training of the ANN is achieved, the corresponding ANN generated weight-file can be easily used by an appropriate subroutine of the main data analysis program for determining the energy of γ -ray like events. Use of a dedicated ANN software package is thus necessary only during the training of the ANN. Hence, compared to the conventional methods, the ANN-based energy reconstruction procedure offers several advantages like reasonably good energy resolution, applicability over a wider zenith angle range and implementation ease.

6 Energy spectrum of the Crab Nebula as measured by the TACTIC telescope

In order to test the validity of the ANN-based energy estimation procedure, we have applied this procedure for determining the energy spectrum of the Crab Nebula. For this purpose we reanalyzed the Crab Nebula data collected by the TACTIC imaging telescope for ~ 101.44 h during Nov. 10, 2005 - Jan. 30, 2006. The zenith angle of the observations was $\leq 45^\circ$. The data has been collected with inner 225 pixels ($\sim 4.5^\circ \times 4.5^\circ$) of the full imaging camera with the innermost 121 pixels ($\sim 3.4^\circ \times 3.4^\circ$) participating in the trigger. The data recorded by the telescope was corrected for inter-pixel gain variation and then subjected to the standard two-level image 'cleaning' procedure with picture and boundary thresholds of 6.5σ and 3.0σ , respectively. The clean Cherenkov images were characterized by calculating their standard image parameters like LENGTH, WIDTH, DISTANCE, ALPHA, SIZE and FRAC2 [4,5]. Before determining the energy spectrum, the agreement between the predictions from Monte Carlo simulations and the actual performance of the telescope has been checked. This is done by comparing the observed trigger rate of the telescope with the predicted value and by comparing the expected and observed image parameter distributions for protons [35]. Reasonably good matching is seen between the experimentally observed quantities and those predicted by simulations.

The standard Dynamic Supercuts procedure [13,31] is used to separate γ -ray like images from the background cosmic rays. The Dynamic Supercuts γ -ray selection criteria used in the present analysis are slightly less tight than the ones used by us in our earlier work [31,32] as the main aim here is to increase the number of γ -ray like events with only a marginal loss of statistical significance. The new cuts values used for the present analysis are the following : $0.11^\circ \leq LENGTH \leq (0.260 + 0.0265 \times \ln S)^\circ$, $0.06^\circ \leq WIDTH \leq (0.110 + 0.0120 \times \ln S)^\circ$, $0.52^\circ \leq DISTANCE \leq 1.27^\circ \cos^{0.88} z$, $SIZE \geq 450d.c$ (where 6.5 digital counts $\equiv 1.0$ pe), $ALPHA \leq 18^\circ$ and $FRAC2 \geq 0.35$. The number of γ -ray events obtained after applying the above cuts are determined to be $\sim (928 \pm 100)$ with a statistical significance of $\sim 9.40\sigma$. Defining $ALPHA \leq 18^\circ$ as the γ -ray domain and $27^\circ \leq ALPHA \leq 81^\circ$ as the background region, the number of γ -ray events have been calculated by subtracting the expected number of background events (calculated on the basis of background region) from the γ -ray domain events.

The differential photon flux per energy bin has been computed using the formula

$$\frac{d\Phi}{dE}(E_i) = \frac{\Delta N_i}{\Delta E_i \sum_{j=1}^5 A_{i,j} \eta_{i,j} T_j} \quad (5)$$

where ΔN_i and $d\Phi(E_i)/dE$ are the number of events and the differential flux at energy E_i , measured in the i th energy bin ΔE_i and over the zenith angle range

of 0° - 45° , respectively. T_j is the observation time in the j th zenith angle bin with corresponding energy-dependent effective area ($A_{i,j}$) and γ -ray acceptance ($\eta_{i,j}$). The 5 zenith angle bins ($j=1-5$) used are 0° - 10° , 10° - 20° , 20° - 30° , 30° - 40° and 40° - 50° with effective collection area and γ -ray acceptance values available at 5° , 15° , 25° , 35° and 45° . The number of γ -ray events (ΔN_i) in a particular energy bin is calculated by subtracting the expected number of background events, from the γ -ray domain events. The γ -ray differential spectrum obtained after using appropriate values of effective collection area and γ -ray acceptance efficiency (along with their energy and zenith angle dependence) is shown in Fig.9a.

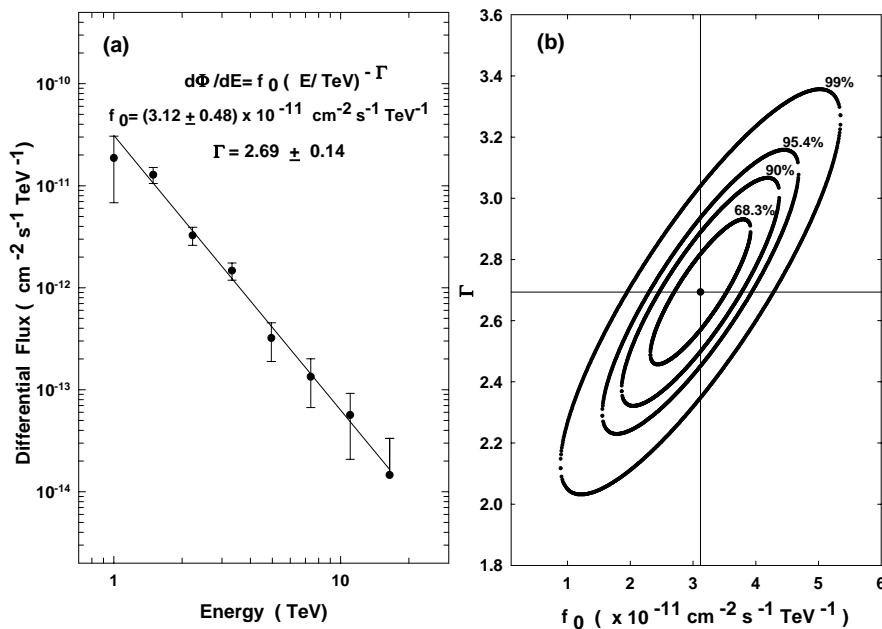


Fig. 9.

A power law fit ($d\Phi/dE = f_0 E^{-\Gamma}$) to the measured differential flux data with $f_0 \sim (3.12 \pm 0.48) \times 10^{-11} \text{ cm}^{-2} \text{ s}^{-1} \text{ TeV}^{-1}$ and $\Gamma \sim 2.69 \pm 0.14$ is also shown in Fig.9a. The fit has a $\chi^2/dof \sim 3.64/6$ with a corresponding probability of ~ 0.72 . The errors in the flux constant and the spectral index are standard errors. Reasonably good matching of this spectrum with that obtained by the Whipple and HEGRA groups [45,46] reassures that the procedure followed by us for obtaining the energy spectrum of a γ -ray source is quite reliable. The confidence ellipses in the two parameters jointly (i.e f_0 and Γ) at 68.3%, 90%, 95.4% and 99% confidence levels are shown in Fig.9b. The corresponding $\Delta\chi^2$ values of these 4 contours, for 6 degrees of freedom are ~ 7.04 , ~ 10.6 , ~ 12.8 and ~ 16.8 .

It is important to point out here that for background cosmic ray events, which are not coming from the source direction and are classified as γ -ray like events by the Dynamic Supercuts procedure, a wrong energy value will be obtained for them.

However, subtraction of the background events (estimated from $27^\circ \leq \text{ALPHA} \leq 81^\circ$ region), from the γ -ray domain (defined as $\alpha \leq 18^\circ$), will cancel out these events (in a statistical sense). Estimating the energy spectrum of γ -rays in the presence of background events by following this approach is well known [39] and has been used quite extensively by other groups.

7 Conclusions

A novel ANN-based energy estimation procedure, for determining the energy spectrum of a candidate γ -ray source has been developed. The procedure followed by us uses an Artificial Neural Network to estimate the energy of a γ -ray like event on the basis of its image SIZE, DISTANCE and zenith angle. Apart from yielding a reasonably good $\sigma(\Delta_E)$ of $\sim 26\%$, this procedure has the added advantage that it allows data collection over a much wider zenith angle range as against a coverage of upto 30° only in case the zenith angle dependence is to be ignored. We have also successfully implemented the ANN-based energy reconstruction algorithm in our analysis chain, by directly using the ANN generated weight-file, so that the energy of a γ -ray like event could be predicted without using the ANN software package. Reasonably good matching of the Crab Nebula spectrum as measured by the TACTIC telescope with that obtained by the Whipple and HEGRA groups reassures that the procedure followed by us for obtaining the energy spectrum of a γ -ray source is quite reliable.

8 Acknowledgements

The authors would like to convey their gratitude to all the concerned colleagues of the Astrophysical Sciences Division for their contributions towards the instrumentation and observation aspects of the TACTIC telescope. The authors would also like to thank Sh. N. Bhatt for helpful discussions related to Section 6 of this work.

References

- [1] P.M. Chadwick, I.J.Latham, S.J.Nolan, J.Phys. G. Nucl. Part. Phys. 35 (2008) 033201.
- [2] A.De Angelis, O.Mansutti, M.Persic, Nuovo Cimento 31 (2008) 187.
- [3] F. Aharonian, J.Buckley, T.Kifune, G.Sinnis, Rep. Prog. Phys. 71 (2008) 096901.
- [4] A.M. Hillas, Proc. 19th. ICRC, La Jolla. 3 (1985) 445.
- [5] D.J. Fegan, Space Science Reviews. 75 (1996) 137.

- [6] T.C. Weekes et al., *Ap.J.* 342 (1989) 379.
- [7] E. Lorentz et al., *New Astron. Rev.* 48 (2004) 339.
- [8] T.C. Weekes et al., *Astropart. Phys.* 17 (2002) 221.
- [9] J.A. Hinton et al., *New Astron. Rev.* 48 (2004) 331.
- [10] H. Kubo et al., *New Astron. Rev.* 48 (2004) 323.
- [11] F.A. Aharonian et al., *Nature.* 440 (2006) 1018.
- [12] J. Albert et al., *Science.* 320 (2008) 1752.
- [13] G. Mohanty et al., *Astropart. Phys.* 9 (1998) 15.
- [14] F. Aharonian et al., *Astron. Astrophys.* 349 (1999) 29.
- [15] P.F. Rebillot et al., *Ap.J.* 641 (2006) 740.
- [16] F.A. Aharonian et al., *Astropart. Phys.* 6 (1997) 343.
- [17] F.A. Aharonian et al., *Astropart. Phys.* 6 (1997) 369.
- [18] L. Lonnblad et al., *Phys. Rev. Lett.* 65 (1990) 1321.
- [19] C. Bortolotto et al., *Nucl. Instr. and Meth. A.* 306(1991) 459
- [20] P. Abreu et al., *Phys. Lett. B* 295 (1992) 383
- [21] B. Brandl et al., *Nucl. Instr. and Meth. A.* 324(1993) 307
- [22] R. Borisjuk et al., *Nucl. Instr. and Meth. A.* 381 (1996) 512.
- [23] J. Damgov and L.Litov, *Nucl. Instr. and Meth. A.* 482 (2002) 776.
- [24] P.V.M. da Silva and J.M. de Seixas, *Nucl. Instr. and Meth. A.* 559 (2006) 124.
- [25] R.A. Vazquez, F.Halzen and E.Zas, *Phy. Rev. D.* 45 (1992) 356.
- [26] P.T. Reynolds, *Irish Astron. J.* 21 (1993) 118.
- [27] P.T. Reynolds and D.J.Fegan, *Astropart. Phys.* 3 (1995)137.
- [28] P. Boinee, A.De Angelis and G.L.Foresti, *Proc. World Academy of Science, Engineering and Technology*, 7 (2005)394
- [29] D. Dumora et al., *Nucl. Phys. B (Proc. Suppl.)* 97 (2001) 255.
- [30] R.K. Bock et al., *Nucl. Instr. and Meth. A.* 516 (2004) 511.
- [31] K.K. Yadav et al., *Astropart. Phys.* 27 (2007) 447.
- [32] S.V. Godambe et al., *J.Phys. G. Nucl. Part. Phys.* 35 (2008) 065202.
- [33] S.R. Kaul et al., *Nucl. Instr. and Meth. A.* 496 (2003) 400.
- [34] K.K. Yadav et al., *Nucl. Instr. and Meth. A.* 527(2004) 411.

- [35] R. Koul et al., Nucl. Instr. and Meth. A. 578 (2007) 548.
- [36] D. Heck et al., Report FZKA 6019 Forschungszentrum, Karlsruhe. (1998).
- [37] M. Lemoine-Goumard, B.Degrange and M.Tluczykont, Astropart. Phys. 25 (2006) 195.
- [38] F. Aharonian et al., Astron. Astrophys. 457 (2006) 899.
- [39] W. Hofmann et al., Astropart. Phys. 12 (2000) 207.
- [40] T. Schweizer, Ph.D Thesis, Universitat Autònoma de Barcelona, (2002)
- [41] R. Tagliaferri et al., Neural Networks. 16 (2003) 297.
- [42] J.M. Zurada, Introduction to Artificial Neural Systems, Jaico Publishing House, Mumbai, 2006.
- [43] M. Reidmiller, Computer Standards Interfaces. 16 (1994) 265.
- [44] R.O. Duda, P.E.Hart and D.G.Stork, Pattern Classification, John Wiley And Sons, New York, 2002.
- [45] A.M. Hillas et al., Ap.J, 503 (1998) 744.
- [46] F.A. Aharonian et al., Ap.J, 614 (2004) 897.

9 Figure Captions

Fig 1. Variation of $\langle \text{SIZE} \rangle$ as a function of $\langle \text{DISTANCE} \rangle$ for γ -rays from a point source of different energies at zenith angles of (a) 15° and (b) 35° .

Fig 2. Variation of $\langle \text{DISTANCE} \rangle$ as a function of core distance for γ -rays of various energies from a point source at zenith angles of (a) 15° and (b) 35° .

Fig 3. (a) Relative mean error in the reconstructed energy ($\Delta_E = (E_{estm} - E_{true})/E_{true}$) as a function of energy for zenith angle of 25° using the energy estimation procedure given by equation (1). Relative mean error in the estimated energy as a function of energy for zenith angles of (b) 15° and (c) 35° if zenith angle dependence is ignored in the energy reconstruction procedure.

Fig 4. (a) Relative mean error in the reconstructed energy ($\Delta_E = (E_{estm} - E_{true})/E_{true}$) as a function of energy for the energy estimation procedure given by equation (2). (b) Frequency distribution of Δ_E along with a best fit Gaussian distribution to the data.

Fig 5. (a) Relative mean error in the reconstructed energy ($\Delta_E = (E_{estm} - E_{true})/E_{true}$) as a function of energy for the look-up table based energy estimation procedure. (b) Frequency distribution of Δ_E along with a best fit Gaussian distribution to the histogram.

Fig 6. (a) Normalised root mean square error as a function of number of nodes in the hidden layer. (b) Normalised root mean square error as a function of number of iterations for 30 nodes in the hidden layer.

Fig 7. (a) Relative mean error in the reconstructed energy ($\Delta_E = (E_{estm} - E_{true})/E_{true}$) as a function of energy for the ANN- based energy estimation procedure. (b) Frequency distribution of Δ_E along with a best fit Gaussian distribution to the histogram.

Fig 8. (a) Relative mean error in the reconstructed energy ($\Delta_E = (E_{estm} - E_{true})/E_{true}$) as a function of energy for the ANN- based energy estimation procedure when applied to a validation data sample. (b) Frequency distribution of Δ_E along with a best fit Gaussian distribution to the histogram..

Fig 9. (a) The differential energy spectrum of the Crab Nebula as measured by the TACTIC telescope and employing the ANN-based energy reconstruction procedure. (b) The confidence ellipses in the two parameters jointly (i.e f_0 and Γ) at 68.3%, 90%, 95.4% and 99% confidence levels.